

Magnetic Correlations in Nanostructured Ferromagnets

Jörg F. Löffler,^{1,2} Hans-Benjamin Braun,¹ and Werner Wagner¹

¹*Paul Scherrer Institut, CH-5232 Villigen PSI, Switzerland*

²*W.M. Keck Laboratory, California Institute of Technology, Pasadena, California 91125*

(Received 22 February 2000)

Small-angle neutron scattering experiments on nanostructured Fe, Co, and Ni reveal grain-size dependent magnetic correlations across grain boundaries. In Fe, a minimum of the correlation length is observed for grain sizes of the order of the bulk domain-wall width where the coercive field has a maximum. The results are explained within a generalization of the random-anisotropy model that takes into account domain-wall formation within grains and reduced interface coupling.

PACS numbers: 75.50.Kj, 61.12.Ex, 75.10.Nr, 75.60.Ch

Nanostructured materials often reveal macroscopic properties that strikingly differ from their bulk counterparts: A granular metal can be mechanically hard compared to the bulk material for grain sizes in the micron range, but the same compound can surprisingly turn soft when the grains reach the size of a few nanometers [1,2].

A similar situation arises for magnetic materials. Isolated nanoparticles [3] above the onset of superparamagnetism are magnetically hard, i.e., they have a large coercivity. In contrast, nanostructured magnets consisting of densely packed grains are often magnetically soft as a result of the interaction between the grains. Their superior soft magnetic properties render these materials [4] ideal for applications such as transformer sheets. Quite remarkably, the coercivity in such materials can be tuned by variation of the grain size. It shows a distinct maximum at grain sizes of typically some tens of nanometers, falling off sharply towards smaller grains [5].

In order to design magnetic materials for specific applications, it is important to understand how such macroscopic properties arise from the interplay of microscopic parameters such as grain size, intergrain coupling, and anisotropies. Furthermore, for the continuous increase of magnetic storage density, it is crucial to know to what extent the independence of individual storage units can be maintained in the presence of interparticle coupling.

An important step in relating microscopic and macroscopic properties has been taken in Ref. [5]. The grain size dependence of the magnetic properties of nanostructured materials has been related to the so called random-anisotropy model (RAM) [6,7], the random anisotropy being caused by the random orientation of the individual grains. In this model, the ferromagnetic long-range order is destroyed for arbitrarily weak random anisotropies in dimensions $d \leq 4$ even at zero temperature, analogous to the loss of long-range order in the random-field model by Imry and Ma [8]. Both models predict an increase of magnetic correlations with decreasing correlation length of the random perturbations. If such a description were indeed adequate for nanostructured ferromagnetic materials, one would observe a corresponding increase of the correlation

length with decreasing grain size, accompanied by a decrease in coercivity even for a single material.

In order to resolve the interplay of structure and magnetic correlations at the nanoscale, we performed small-angle neutron scattering (SANS) experiments on nanostructured Fe, Co, and Ni with different grain sizes (10–100 nm) and anisotropy. In Fe and Ni, the magnetic correlations extend over many grains. Furthermore, in Fe, we observe a minimum of the correlation length for grain sizes near the domain-wall width, mirrored by a maximum of the coercive field. In (hcp) Co with strong crystalline anisotropy, the observed correlation lengths are of the order of the grain size. To explain these results, we introduce a generalization of the RAM that takes into account the peculiar features of a real nanostructured magnet: The exchange across grain boundaries can be considerably weaker than the intragrain exchange; further, the uniform anisotropy within one grain may lead to the formation of domain walls.

The nanostructured samples were produced by the inert-gas condensation technique [9], i.e., by evaporation of the raw material and condensation in He atmosphere, followed by consolidation by pressing. This produces solid, disk-shaped, metallic samples of 8 mm diameter, 100–300 μm thickness, and grain sizes of approximately 10 nm. The grain size was increased incrementally up to 100 nm by thermal annealing. The SANS measurements were carried out at the instrument V4 of Hahn-Meitner-Institut, Berlin, using a neutron wavelength of $\lambda = 8 \text{ \AA}$ with spread $\Delta\lambda/\lambda = 0.1$. The measurements were performed at room temperature with the samples placed in a homogenous, horizontal field of up to 10 kOe, parallel to the flat surfaces of the nanostructured samples. The data were corrected for background, transmission, and geometric effects, and normalized to obtain the scattering on an absolute scale.

Figure 1 shows examples of the radial scattering cross section for as-prepared Fe, Co, and Ni, measured in zero field and a field of 10 kOe. The corresponding radial scattering curves lie closely together and are parallel for large Q values; for smaller Q a significant splitting is observed,

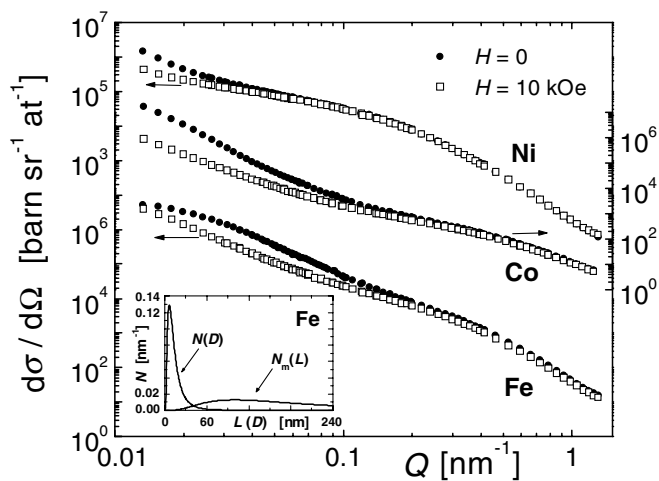


FIG. 1. Radial scattering cross section for as-prepared nanostructured Fe, Co, and Ni, measured at $H = 0$ and $H = 10$ kOe as a function of the scattering vector Q [$Q = 4\pi\sin\theta/\lambda$ with $\theta = \text{half the scattering angle}$]. Inset: grain size distribution $N(D)$ and size distribution of magnetic correlation lengths, $N_m(L)$, for as-prepared Fe [$D = 12$ nm].

which occurs at the highest Q value for Co (having the highest bulk anisotropy), and shifts to lower values for Fe and Ni. The splitting of the SANS intensity owing to an additional scattering in zero field reflects magnetic correlations which are considerably larger than the grain size of approximately 10 nm in the as-prepared state. These measurements therefore give evidence that at $H = 0$ spontaneous magnetic correlations form, which extend over several grains. Such correlations were also found in other SANS studies [10,11], but without an investigation of the grain size dependence.

For the quantitative analysis of our SANS data, we followed the data evaluation procedure applied in Ref. [10]. In an external field of 10 kOe the magnetization is close to saturation as was confirmed by additional measurements in fields of 60 kOe. Thus, the scattering at 10 kOe originates from the contrast of magnetically aligned grains against grain boundaries. After performing an angular average in the detector plane, we obtain the radial scattering cross section

$$\frac{d\sigma}{d\Omega} = \left[\frac{1}{2} (\Delta b_m)^2 + (\Delta b_n)^2 \right] i_p(Q), \quad (1)$$

where Δb_m and Δb_n are the corresponding differences of magnetic and nuclear scattering lengths. The structure function $i_p(Q)$ is that of a collection of grains averaged over the size distribution. In zero magnetic field, the magnetization of all grains is no longer aligned, as reflected by the low remanence with $M_r/M_s \approx 0.05-0.1$. The corresponding radial scattering cross section is then

$$\frac{d\sigma}{d\Omega} = \left[\frac{2}{3} (\Delta b_m)^2 + (\Delta b_n)^2 \right] i_p(Q) + \frac{2}{3} (\Delta b_m)^2 i_c(Q), \quad (2)$$

where the first two terms arise again from the scattering contrast of grains against grain boundaries. The prefactor of the magnetic term, however, results now from averaging over arbitrary magnetization directions; i_c is the structure function of the now existing intergranular magnetic correlations. In Eqs. (1) and (2) we have neglected interparticle correlations since the grains are randomly distributed and no short-range order exists.

From our SANS measurements in a field of 10 kOe and Eq. (1) we obtain the grain size distribution $N(D)$ of our samples. Following transmission electron microscopy investigations, we assumed $N(D)$ to be log-normally distributed and the particle shape to be approximately spherical [12]; cf. inset of Fig. 1. The volume-weighted average grain size $D = \langle D \rangle_N$ agrees well with the average grain size obtained from x-ray diffraction using the method of Ref. [13]. [$\langle \cdot \rangle_N$ denotes the expectation value with respect to $N(D)$]. The intergranular magnetic correlations were derived from the extra magnetic scattering in zero field by subtracting the scattering cross section at 10 kOe (1) from that at zero field (2). In order to account for the different prefactors, the scattering at 10 kOe was multiplied by a constant factor to match both scattering cross sections at large Q . The size distribution of the magnetic correlations $N_m(L)$ was calculated analogously to $N(D)$, assuming spherical correlation volumes. For as-prepared Fe, the resulting $N_m(L)$ is shown in the inset of Fig. 1.

An analysis of the data for as-prepared Fe, Co, and Ni shows that the smallest correlation lengths are found in (hcp) Co, down to around 20 nm [14]. The largest magnetic correlations have been observed in Ni, where they exceed 150 nm and are near the resolution limit of the experiment. The increase of the correlation lengths of the different materials is consistent with an increase of the corresponding values of the bulk domain-wall width, which are $\delta_0^{\text{Co}} = (A/K)^{1/2} = 5$ nm, $\delta_0^{\text{Fe}} = 15$ nm, and $\delta_0^{\text{Ni}} = 40$ nm at room temperature, with A the exchange, and K the bulk anisotropy constant.

The inert-gas condensation technique leads to optimally attainable grain sizes of around 15 nm. Since the most dramatic changes of the magnetic properties are expected to occur at $D \approx \delta_0$, we decided to study Fe in more detail. Figure 2 shows the volume-weighted correlation length $L = \langle L \rangle_{N_m}$ for all Fe samples investigated as a function of D . The correlation length L shows a clear minimum for grain sizes in the range of 20–35 nm, similar to the range where the coercivity has a maximum [15]. The observed increase of the correlation length with decreasing grain sizes indicates a coupling between adjacent grains and is consistent with the RAM. This increase cannot be explained by dipolar interactions between uniformly magnetized grains, since the dipolar energy density then scales with the grain size and thus would lead to a decrease of the correlation length.

On the other hand, the original version of the RAM [7] is unable to explain the crossover of the magnetic properties as it does not take into account the granular structure of

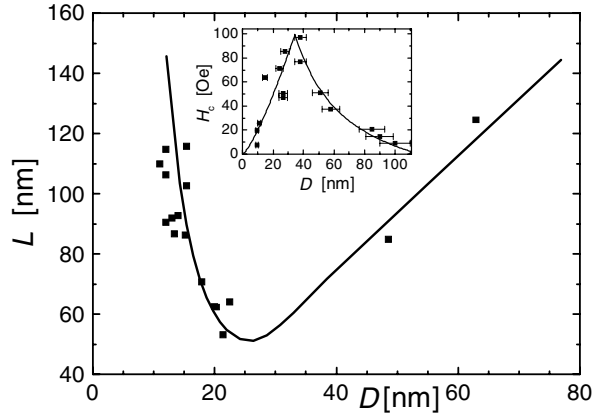


FIG. 2. Magnetic correlation length $L = \langle L \rangle_{N_m}$ versus grain size $D = \langle D \rangle_N$ for nanostructured Fe. The solid line is obtained from Eq. (9) with $\delta_{\text{eff}}^{\text{Fe}} = 18$ nm and $\lambda = 2$. For comparison, the inset shows the coercivity, H_c , versus grain size (from Ref. [15]).

the material. We therefore propose a generalization of the RAM that includes reduced intergrain coupling and allows for the disruption of magnetic order due to the creation of domain walls within grains, as suggested by numerical simulations [16]. Explicitly, we consider the following generalized RAM, with energy

$$E = A \sum_{i,\alpha} \int_{V_i} d^3x (\nabla m_i^\alpha)^2 - K \sum_i \int_{V_i} d^3x (\mathbf{m}_i \cdot \mathbf{n}_i)^2 - \sum_{\langle i,j \rangle} \frac{I_{ij}}{d} \int_{S_{ij}} d^2x \mathbf{m}_i \cdot \mathbf{m}_j, \quad (3)$$

where $\mathbf{m}_i(\mathbf{x})$ denotes the space dependent magnetization unit vector within grain i of volume V_i , and \mathbf{n}_i is the unit vector of the random anisotropy of strength $K > 0$, A is the intragrain exchange constant, and $I_{ij} > 0$ characterizes the (reduced) random, ferromagnetic exchange across the interfaces S_{ij} of width d . The latter term is new here and allows for magnetization discontinuities across grain boundaries. The above model reduces to the traditional RAM in two limits: For $I_{ij} = A$ and with d the lattice constant, the exchange is uniform, and for $D^2 < A/K$ we recover the RAM with a correlation length of the randomness that corresponds to the grain size. On the other hand, for $I_{ij}D/d < KD^2 < A$, the grains play the role of randomly coupled large spins. Introducing the projection of the magnetization onto the anisotropy axis $\mathbf{m}_i = \tau_i \mathbf{n}_i$ with $\tau_i = \pm 1$, the above model with $I_{ij} = I$ is equivalent to a random-bond Ising model with biased exchange having spin glass properties in 3D [17]. These arguments in conjunction with Ref. [18] may provide an additional explanation for the observed difference between zero-field cooled and field cooled susceptibilities [19,15] that is commonly attributed to a spin glass phase at grain surfaces.

Some basic features of our model such as the crossover of magnetic properties at grain sizes $D \approx \delta_0$ can be studied by considering the exactly solvable case of two coupled grains $\chi = \pm$. The anisotropy axes \mathbf{n}_+ , \mathbf{n}_- span the plane

of the equilibrium magnetization, and the magnetization in each grain is characterized by the angle θ_χ which is chosen such that the anisotropy axes are at $\theta_\chi = \chi\alpha/2$. The energy per area is then given by

$$\mathcal{E} = \sum_{\chi=\pm} \int_{D_\chi} dx \left\{ A(\partial_x \theta_\chi)^2 + K \sin^2\left(\theta_\chi - \chi \frac{\alpha}{2}\right) \right\} - (I/d) \cos(\theta_+^0 - \theta_-^0), \quad (4)$$

where $\theta_\chi(x)$ is defined on the range D_χ with $0 < \chi x < D$, and θ_χ^0 is the interface value. The magnetization is assumed to obey free boundary conditions on all surfaces except the interface. Assuming two cubic grains of same size, $\theta_- = -\theta_+$, and $\partial_x \theta_\chi = 0$ at $x = \chi D$. Note that the energy (4) also describes the magnetization near the interface of two arbitrarily shaped grains, with x the coordinate normal to the interface. Integration of the Euler-Lagrange equations leads to $(A/K)(\partial_x \theta_\chi)^2 + \cos^2(\theta_\chi - \chi\alpha/2) = k^2$ with $0 < k < 1$. In addition, at the interface we have $A\partial_x \theta_-^0 = (I/d) \sin 2\theta_+^0$, and $\partial_x \theta_-^0 = \partial_x \theta_+^0$. For arbitrary grain size and interface coupling we then obtain the magnetization profile,

$$\tan \frac{\alpha/2 - \theta_+(x)}{2} = \sqrt{\frac{1-k}{1+k}} / \text{dn}\left(\frac{x-D}{\delta}, \tilde{k}\right), \quad (5)$$

where $\text{dn}(x, \tilde{k})$ denotes the Jacobian elliptic function of modulus $\tilde{k} = 2\sqrt{k}/(1+k)$, and $\delta = 2\delta_0/(1+k)$ with $\delta_0 = \sqrt{A/K}$. Considering the interface slip angle θ_+^0 as a parameter it follows that $k^2 = \cos^2(\theta_+^0 - \alpha/2) + \rho^2 \sin^2 2\theta_+^0$, and $k = \cos(\theta_+^0 - \alpha/2)$. The grain size D is obtained by evaluating Eq. (5) at the interface $x = 0$.

For large grains, $D \gg \delta_0$, the magnetization rapidly approaches the easy-axis direction away from the interface. For small intergrain coupling, this occurs via an abrupt phase slip near the interface, while for large coupling this transition occurs within a boundary layer of width δ_0 ; cf. Fig. 3. The strength of the intergrain coupling is controlled by the parameter $\rho \equiv I\delta_0/Ad$, the ratio between interface wall energy and domain wall energy within a grain. We conclude that for D/δ_0 large, the magnetization is *never* transferred coherently between adjacent grains and consequently,

$$L = \lambda D. \quad (6)$$

In contrast to the random-field case, the equilibrium magnetization in two neighboring grains with uniaxial anisotropy will at most deviate within a hemisphere, and $\langle \mathbf{m}_i \cdot \mathbf{m}_j \rangle_n = 1/2$ for i, j nearest neighbors. With an exponential decay of correlations, this implies $\lambda \approx 2$.

For small grain sizes $D < \delta_0$, the magnetization overrides the local anisotropy. Remarkably, this even occurs for small intergrain coupling ρ at sufficiently small grain sizes. In this regime, the correlations extend over several grains, a behavior familiar from random-field model and RAM [7,8]. The correlation length results from the balance between the anisotropy-energy gain within a finite volume element, and the cost of exchange energy for adjusting the magnetization between such volume elements. Computing

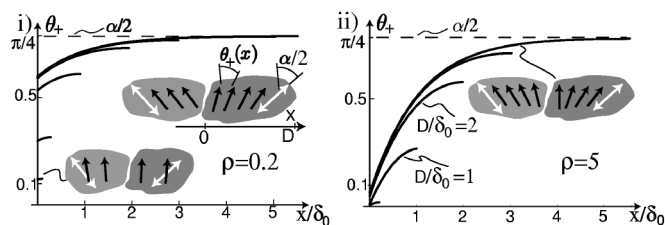


FIG. 3. Magnetization configuration (5) of two coupled grains as a function of grain size D for (i) weak ($\rho = 0.2$) and (ii) strong ($\rho = 5$) intergrain coupling for $\alpha = \pi/2$. The inset depicts two grains and the relevant coordinate axis. For large grains, $D/\delta_0 > 1$, a domain wall is created either (i) as a phase slip directly at the interface or (ii) as a domain wall extending into the grain. At small grain sizes, $D/\delta_0 < 1$, the magnetization (dark arrows) overrides the intragrain anisotropy (bright arrows), and the RAM or its generalized version applies.

the energy involved in applying a twist to the opposite faces of a cubic region of size $L = N(D + d)$ with N cubic grains leads to the effective exchange constant,

$$A_{\text{eff}} = A(1 + d/D)/(1 + Ad/ID). \quad (7)$$

Note that this expression interpolates between the uniform case $I = A$, where $A_{\text{eff}} = A$, and the case of soft interfaces, where $A_{\text{eff}} \approx ID/d$ with the twist being absorbed by the interfaces. The energy density for the magnetization to adjust over a region of size L is given by $A_{\text{eff}}L^{-2} - K(D/L)^{3/2}$, derived in close analogy to the RAM. Minimization with respect to L leads to the correlation length for the generalized RAM

$$L = (16/9)\delta_{\text{eff}}^4/D^3, \quad (8)$$

with $\delta_{\text{eff}} = (A_{\text{eff}}/K)^{1/2}$. We thus obtain the important result that, for small grains with $D < \delta_0$, the RAM applies for weak intergrain coupling as long as $ID/Ad \geq 1$.

Motivated by the rather sharp crossover between the regimes of small and large grains illustrated by Eq. (5) and Fig. 3, we assume that small grains contribute to a correlation length via the generalized RAM, whereas larger grains follow relation (6). The domain size distribution is then given by

$$N_m(L) = \{\Theta(D_c - D)N(D)|dD/dL|\}_{D_{\text{RAM}}(L)} + \{\Theta(D - D_c)N(D)|dD/dL|\}_{D_\lambda(L)}, \quad (9)$$

where $D_{\text{RAM}}(L)$ and $D_\lambda(L)$ denote the use of Eqs. (8) and (6), respectively; $D_c = (16/9\lambda)^{1/4}\delta_{\text{eff}}$ is the crossover grain size, and Θ is the step function. From the measured log-normal distribution $N(D)$, Eq. (9) allows us to compute the domain size distribution. In Fig. 2, the Fe data are compared with the correlation length $L = \langle L \rangle_{N_m}$, computed from Eq. (9) with $\delta_{\text{eff}}^{\text{Fe}} = 18$ nm and $\lambda = 2$. Comparing this to $\delta_0^{\text{Fe}} = 15$ nm, we conclude that $A_{\text{eff}} \approx A$ and thus $Ad/ID \ll 1$, at least for a number of intergrain

couplings exceeding the percolation threshold of cluster size L .

The observations on Ni and Co are also in accordance with our model; all investigated Ni samples had grain size $D = 14$ to 22 nm ($< \delta_0^{\text{Ni}} = 40$ nm) and showed magnetic correlations exceeding 150 nm, in accordance with Eq. (9) which predicts correlations dominated by the RAM (8). In contrast, for the available (hcp) Co samples with $D = 7$ to 70 nm ($> \delta_0^{\text{Co}} \approx 5$ nm), the observed magnetic correlations were always of the order of the grain size, as predicted by Eqs. (6) and (9).

In conclusion, we have found that in various nanostructured materials the magnetic correlations show significantly different behavior for grain sizes below and above a domain-wall width. We have determined the minimum intergrain exchange coupling required for intergrain correlations. Furthermore, we have derived a relation which allows us to predict the domain size distribution for given grain size distributions, exchange, and anisotropy constants. It would be interesting to observe similar effects in nanolithographic systems or in granular thin films.

Support by the Swiss National Science Foundation and by the Alexander von Humboldt Foundation via the Feodor Lynen Program (J. L.) is gratefully acknowledged.

-
- [1] S. Yip, *Nature (London)* **391**, 532 (1998); A.H. Chokshi *et al.*, *Scr. Metall.* **23**, 1679 (1989).
 - [2] *Nanomaterials: Synthesis, Properties and Applications*, edited by A.S. Edelstein and R.C. Cammarata (Institute of Physics Publishing, Philadelphia, 1996).
 - [3] W. Wernsdorfer *et al.*, *Phys. Rev. Lett.* **78**, 1791 (1997); for inelastic neutron scattering, see M.F. Hansen *et al.*, *Phys. Rev. Lett.* **79**, 4910 (1997).
 - [4] Y. Yoshizawa *et al.*, *J. Appl. Phys.* **64**, 6044 (1988).
 - [5] G. Herzer, *J. Magn. Magn. Mater.* **112**, 258 (1992).
 - [6] R. Harris *et al.*, *Phys. Rev. Lett.* **31**, 160 (1973).
 - [7] R. Alben *et al.*, *J. Appl. Phys.* **49**, 1653 (1978); E.M. Chudnovsky *et al.*, *Phys. Rev. B* **33**, 251 (1986).
 - [8] Y. Imry and S.K. Ma, *Phys. Rev. Lett.* **35**, 1399 (1975).
 - [9] H. Gleiter, *Prog. Mater. Sci.* **33**, 223 (1989).
 - [10] W. Wagner *et al.*, *J. Mater. Res.* **6**, 2305 (1991).
 - [11] J. Weissmüller *et al.*, *Mater. Res. Soc. Symp. Proc.* **457**, 231 (1998).
 - [12] V. Haas and R. Birringer, *Nanostruct. Mater.* **1**, 491 (1992).
 - [13] H.P. Klug and L.E. Alexander, *X-ray Diffraction Procedures for Polycrystalline and Amorphous Materials* (Wiley, New York, 1974), 2nd ed., pp. 661–665.
 - [14] X-ray diffraction of Co revealed the existence of some fcc particles with much smaller anisotropy. The additional zero-field scattering for Co at small Q (Fig. 1) is due to the scattering of such magnetically correlated grains.
 - [15] J.F. Löffler *et al.*, *Phys. Rev. B* **57**, 2915 (1998).
 - [16] T. Schrefl *et al.*, *Phys. Rev. B* **49**, 6100 (1994).
 - [17] A. J. Bray and M. Moore, *J. Phys. C* **18**, L139 (1985).
 - [18] C. Djurberg *et al.*, *Phys. Rev. Lett.* **79**, 5154 (1997).
 - [19] R. Kodama *et al.*, *Phys. Rev. Lett.* **77**, 394 (1996); E. Bonetti *et al.*, *Phys. Rev. Lett.* **83**, 2829 (1999).